Journal of Organometallic Chemistry 731 (2013) 67–72

Contents lists available at SciVerse ScienceDirect

Journal of Organometallic Chemistry

journal homepage: www.elsevier.com/locate/jorganchem

Regioselective cyclometallation of 4-*R*-1-naphthaldehyde benzoylhydrazones: Palladium(II) complexes with CNO pincer like ligands

A.R. Balavardhana Rao, Samudranil Pal*

School of Chemistry, University of Hyderabad, Hyderabad 500 046, India

ARTICLE INFO

Article history:
Received 26 December 2012
Received in revised form
8 February 2013
Accepted 11 February 2013

Keywords:
Palladium(II)
Benzoylhydrazone
Cyclopalladation
Peri-metallation
Crystal structure

ABSTRACT

Reactions of Li_2PdCl_4, 4-*R*-1-naphthaldehyde benzoylhydrazones (H_2L^n; $n = 1$ and 2 for R = H and OMe, respectively) and $NaOAc\cdot 3H_2O$ in 1:1:1 mole ratio in methanol provide the cyclopalladated complexes with the general formula $[Pd(HL^n)Cl]$ (**1** (R = H) and **2** (R = OMe)). Treatment of one mole equivalent of $[Pd(HL^n)Cl]$ (**1** and **2**) with two mole equivalents of PPh_3 in acetone results in the deprotonation of the O-coordinated amide functionality and the replacement of the metal coordinated chloride with PPh_3 leading to the formation of $[Pd(L^n)(PPh_3)]$ (**3** and **4**). All the complexes have been characterized with the help of elemental analysis and spectroscopic (IR, UV–vis and ^{1}H NMR) measurements. NMR spectra indicates the *peri*-metallation of the 1-naphthalenyl fragment of the tridentate ligand in **1**–**4**. Molecular structures determined by X-ray crystallography confirm the regioselective *peri*-metallation in each of **2**, **3** and **4**.

1. Introduction

The cyclometallation chemistry and cyclometallated complexes continue to be an area of immense interest during the last few decades because of their widespread applications in a variety of research areas such as catalysis, organic synthesis, asymmetric synthesis, photochemistry and materials chemistry [1–14]. As a consequence, a vast literature on cyclometallated complexes with various ligands containing a variety of aromatic rings that undergo metallation is available [14–19]. Formation of the cyclometallated intermediate is the key step in various alkylation, carbonylation and annulation reactions [20–23]. In recent years, tridentate pincer ligands have attracted lot of attention for the design and synthesis of new metallacycles which are more efficient in their applications in the above mentioned areas [24–35]. We have been working on cyclometallated complexes with tridentate Schiff bases derived from acid hydrazides for quite some time now [36–41]. In these complexes, the planar acid hydrazones act as tridentate aryl-C, azomethine-N and amide-/amidate-O donor ligands and form 5,5- or 6,5-fused chelate rings. This type of coordination mode makes these ligands unsymmetrical pincer like species [30–35]. Cyclometallation of a ligand that has two potential sites for metallation is of particular interest as it provides the scope for controlled synthesis of a regioselective product [40,42,43]. Such regioselectivity can play a decisive role in synthetic organic reactions [21]. Cyclometallated complexes with various bidentate and tridentate ligands containing polycyclic aromatic fragments such as indole-3, 1-naphthalenyl, 9-phenanthryl and 1-perylene have been reported [43–59]. The aromatic part of these ligands provide both *ortho*- and *peri*-positions as the potential sites for metallation. Among the bidentate ligands, majority produce exclusively *ortho*-metallated species [43–49], while few give both *ortho*- and *peri*-metallated complexes [50–52]. On the other hand, the tridentate ligands produce exclusively either *peri*-metallated [40,53–56] or *ortho*-metallated species [47,57–59]. The dominance of *ortho*-metallation over *peri*-metallation in bidentate ligands is attributed to more stable 5-membered than less stable 6-membered cyclometallated ring formation [51,54]. We have studied the chemistry of palladium with the potentially tridentate C,N,O-donor 4-*R*-1-naphthaldehyde benzoylhydrazones (H_2L^n, $n = 1$ and 2 for R = H and OCH_3, respectively) and found regioselective *peri*-metallation of the 1-naphthalenyl fragment of the ligands. Herein, we describe syntheses, characterization and X-ray crystal structures of these *peri*-metallated complexes.

2. Experimental

2.1. Materials

All chemicals used in this work were of analytical grade available commercially and were used as received. The solvents used were purified by standard methods [60].

* Corresponding author. Tel.: +91 40 2313 4829; fax: +91 40 2301 2460.
E-mail addresses: spsc@uohyd.ernet.in, spscuh2000@yahoo.co.in (S. Pal).

0022-328X/$ – see front matter © 2013 Elsevier B.V. All rights reserved.
http://dx.doi.org/10.1016/j.jorganchem.2013.02.007

2.2. Physical measurements

Elemental analysis data were obtained with a Thermo Finnigan Flash EA1112 series elemental analyzer. Jasco-5300 and Thermo Scientific Nicolet 380 FT-IR spectrophotometers were used to record the infrared spectra. Purity verifications of H_2L^1 and H_2L^2 were performed with a Shimadzu LCMS 2010 liquid chromatograph mass spectrometer. Solution electrical conductivities were measured with a Digisun DI-909 conductivity meter. Electronic spectra were collected on Perkin–Elmer Lambda 35 UV/vis and Shimadzu UV3600 UV-vis-NIR spectrophotometers. The NMR spectra were recorded with the help of Bruker 400 and 500 MHz NMR spectrometers.

2.3. Synthesis of H_2L^1

1-Naphthaldehyde (468 mg, 3 mmol) and a few drops of acetic acid were added to an ethanol solution (50 ml) of benzoylhydrazine (408 mg, 3 mmol). The mixture was boiled under reflux for 3 h. The white crystalline solid separated was collected by filtration, washed with ethanol and then dried in air. Yield: 660 mg (80%). Anal. calcd for $C_{18}H_{14}N_2O$: C, 78.81; H, 5.14; N, 10.21. Found: C, 78.96; H, 5.21; N, 10.11. Mass in Me_2NCHO: $m/z = 274$. UV–vis in Me_2NCHO: λ_{max} (nm) ($10^{-3} \times \varepsilon$ (M^{-1} cm^{-1})) = 355sh (7.1), 336 (10.8), 320sh (9.5). ^1H NMR in $(CD_3)_2SO$: δ (ppm) (J (Hz)) = 11.99 (s, 1H, NH), 9.16 (s, 1H, H^9), 8.91 (8) (d, 1H, H^2), 8.03 (m, 4H, H^4, H^5, H^{12}, H^{16}), 7.97 (7) (d, 1H, H^8), 7.70 (8) (t, 1H, H^{14}), 7.63 (m, 3H, H^3, H^{13}, H^{15}), 7.58 (8) (t, 2H, H^6, H^7).

H_2L^2 was prepared in 85% yield from equimolar amounts of 4-methoxy-1-naphthaldehyde and benzoylhydrazine in presence of acetic acid using the same procedure as described for H_2L^1. Anal. calcd for $C_{19}H_{16}N_2O_2$: C, 74.98; H, 5.30; N, 9.20. Found: C, 74.81; H, 5.21; N, 9.36. Mass in Me_2NCHO: $m/z = 304$ mg. UV–vis in Me_2NCHO: λ_{max} (nm) ($10^{-3} \times \varepsilon$ (M^{-1} cm^{-1})) = 370sh (13.6), 350 (22.3), 335sh (20.9), 280sh (6.8). ^1H NMR in $(CD_3)_2SO$: δ (ppm) (J (Hz)) = 11.83 (s, 1H, NH), 9.02 (8) (d, 1H, H^2), 9.00 (s, 1H, H^9), 8.28 (8) (d, 1H, H^5), 7.99 (7) (d, 2H, H^{12}, H^{16}), 7.87 (8) (d, 1H, H^8), 7.71 (8) (t, 1H, H^{14}), 7.62 (7) (d, 2H, H^{13}, H^{15}), 7.57 (8) (t, 2H, H^6, H^7), 7.11 (8) (d, 1H, H^3) 4.05 (s, 3H, OMe).

2.4. Synthesis of [Pd(HL^1)Cl] (**1**)

A mixture of $PdCl_2$ (178 mg, 1 mmol) and LiCl (86 mg, 2 mmol) was taken in methanol (20 ml) and boiled with stirring under reflux for 1 h. It was then cooled to room temperature and filtered. The filtrate was added drop-wise with stirring to a methanol solution (20 ml) of H_2L^1 (275 mg, 1 mmol) and $NaOAc \cdot 3H_2O$ (136 mg, 1 mmol). The mixture was stirred at room temperature for 48 h. The complex precipitated as yellowish-green solid was collected by filtration, washed with methanol and finally dried in air. Yield: 332 mg (80%). Anal. calcd for $PdC_{18}H_{13}N_2OCl$: C, 52.07; H, 3.16; N, 6.75. Found: C, 52.15; H, 3.08; N, 6.85. UV–vis in Me_2NCHO: λ_{max} (nm) ($10^{-3} \times \varepsilon$ (M^{-1} cm^{-1})) = 428 (15.8), 403 (17.6), 382 (13.5), 360sh (8.0), 350sh (6.5), 320 (8.0), 271 (17.3). ^1H NMR in $(CD_3)_2SO$: δ (ppm) (J (Hz)) = 14.05 (s, 1H, NH), 8.92 (s, 1H, H^9), 8.63 (br s, 1H, H^2), 8.23 (8) (d, 1H, H^4), 8.13 (6) (d, 1H, H^5), 8.08 (7) (d, 2H, H^{12}, H^{16}), 7.82 (8) (d, 1H, H^7), 7.72 (8) (t, 1H, H^{14}), 7.67 (8) (t, 1H, H^3), 7.63 (m, 2H, H^{13}, H^{15}), 7.35 (8) (t, 1H, H^6).

The yellowish-green [Pd(HL^2)Cl] (**2**) was synthesized in 80% yield from $PdCl_2$, LiCl, $NaOAc \cdot 3H_2O$ and H_2L^2 (1:2:1:1 mole ratio) by following a procedure very similar to that described for **1**. Anal. calcd for $PdC_{19}H_{15}N_2O_2Cl$: C, 51.26; H, 3.40; N, 6.29. Found: C, 51.36; H, 3.51; N, 6.15. UV–vis in Me_2NCHO: λ_{max} (nm) ($10^{-3} \times \varepsilon$ (M^{-1} cm^{-1})) = 436 (15.9), 412 (20.3), 391 (16.8), 370sh (10.8), 350sh (6.9), 315 (7.8), 270 (16.3). ^1H NMR in $(CD_3)_2SO$: δ (ppm) (J (Hz)) = 14.17 (s, 1H, NH), 8.76 (s, 1H, H^9), 8.68 (br s, 1H, H^2), 8.12 (8) (d, 2H, H^5, H^7), 8.06 (7) (d, 2H, H^{12}, H^{16}), 7.71 (br s, 1H, H^{14}), 7.62 (br s, 2H, H^{13}, H^{15}), 7.31 (8) (t, 1H, H^6), 7.20 (8) (d, 1H, H^3), 4.11 (s, 3H, OMe).

2.5. Synthesis of [Pd(L^1)(PPh_3)] (**3**)

Solid PPh_3 (131 mg, 0.5 mmol) was added to a suspension of [Pd(HL^1)Cl] (**1**) (104 mg, 0.25 mmol) in acetone (10 ml) and the mixture was stirred at room temperature for 24 h. The complex [Pd(L^1)(PPh_3)] (**3**) separated as a yellowish-green solid was collected by filtration, washed with acetone and finally dried in air. Yield: 110 mg (68%). Anal. calcd for $PdC_{36}H_{27}N_2OP$: C, 67.45; H, 4.25; N, 4.37. Found: C, 67.58; H, 4.15; N, 4.26. UV–vis in Me_2NCHO: λ_{max} (nm) ($10^{-3} \times \varepsilon$ (M^{-1} cm^{-1})) = 428 (17.8), 403 (21.4), 383 (17.6), 360sh (11.0), 345sh (8.2), 319 (8.9), 272 (22.7). ^1H NMR in $(CD_3)_2SO$: δ (ppm) (J (Hz)) = 9.07 (s, 1H, H^9), 8.65 (br, s, 1H, H^2), 8.20 (br, s, 2H, H^{12}, H^{16}), 7.56 (m, 22H, H^3, H^4, H^5, H^7, H^{13-15}, Hs of PPh_3), 6.77 (br, s, 1H, H^6). ^{31}P NMR in $(CD_3)_2SO$: δ (ppm) = 25.51.

The yellowish-green [Pd(L^2)(PPh_3)] (**4**) was synthesized in 68% yield from one mole equivalent of [Pd(HL^2)Cl] (**2**) and two mole equivalents of PPh_3 using a very similar procedure described above. Anal. calcd for $PdC_{37}H_{29}N_2O_2P$: C, 66.23; H, 4.36; N, 4.17. Found: C, 66.38; H, 4.41; N, 4.07. UV–vis in Me_2NCHO: λ_{max} (nm) ($10^{-3} \times \varepsilon$ (M^{-1} cm^{-1})) = 438 (14.0), 415 (20.8), 394 (17.8), 370sh (11.4), 355sh (6.9), 315sh (7.2), 271 (21.2). ^1H NMR in $(CD_3)_2SO$: δ (ppm) (J (Hz)) = 8.88 (s, 1H, H^9), 8.69 (br s, 1H, H^2), 8.16 (8) (d, 2H, H^5, H^7), 8.01 (6.4) (d, 2H, H^{12}, H^{16}), 7.73 (br s, 4H, H^{14}, *para* ^{1}Hs of PPh_3), 7.63 (m, 2H, H^{13}, H^{15}), 7.45 (m, 12H, *o*,*m* ^{1}Hs of PPh_3), 7.21 (8.4) (d, 1H, H^3), 6.71 (br, s, 1H, H^6), 4.11 (s, 3H, OMe). ^{31}P NMR in $(CD_3)_2SO$: δ (ppm) = 25.49.

2.6. X-ray crystallography

Single crystals of **2** were grown by diethyl ether vapour diffusion into its dimethylformamide solution, while single crystals of **3** and **4** were obtained by slow evaporation of their corresponding acetonitrile solutions. Complex **2** crystallizes as [Pd(HL^2)Cl]·Me_2NCHO (**2**·Me_2NCHO). On the other hand, complexes **3** and **4** crystallize as it is without any solvent molecule. Determination of

Table 1
Selected crystallographic data.

Complex	**2**·$(CH_3)_2NCHO$	**3**	**4**
Chemical formula	$PdC_{22}H_{22}N_3O_3Cl$	$PdC_{36}H_{27}N_2OP$	$PdC_{37}H_{29}N_2O_2P$
Formula weight	518.28	640.97	670.99
Crystal system	Monoclinic	Monoclinic	Monoclinic
Space group	$C2/c$	$P2_1/n$	$P2_1/c$
a (Å)	21.487(3)	16.0972(5)	24.8618(14)
b (Å)	8.9400(12)	15.4471(4)	15.7887(9)
c (Å)	23.968(4)	23.2869(7)	15.4990(9)
β (°)	111.397(5)	102.977(3)	101.218(1)
V (Å^3)	4286.8(11)	5642.5(3)	5967.7(6)
Z	8	8	8
ρ (g cm^{-3})	1.606	1.509	1.494
μ (mm^{-1})	1.019	0.748	0.713
Reflections collected	19,917	27,787	42,467
Reflections unique	3779	9937	10,515
Reflections [$I \geq 2\sigma(I)$]	2952	6511	8226
Parameters	274	739	775
$R1$, $wR2$ [$I \geq 2\sigma(I)$]	0.0560, 0.1107	0.0398, 0.0913	0.0380, 0.0878
$R1$, $wR2$ [all data]	0.0762, 0.1192	0.0694, 0.0998	0.0539, 0.0943
GOF on F^2	1.098	0.907	1.023
Largest diff. peak and hole (e Å^{-3})	0.586, −0.315	1.953, −0.612	0.575, −0.260

unit cell parameters and intensity data collection at 298 K for **2**·Me_2NCHO and **4** were performed with the help of a Bruker-Nonius SMART APEX CCD single crystal diffractometer using graphite monochromated Mo $K\alpha$ radiation (λ = 0.71073 Å). The SMART and the SAINT-Plus packages [61] were used for data acquisition and data extraction, respectively. The SADABS program [62] was used for absorption corrections. Unit cell parameters and the intensity data at 298 K for **3** were obtained using graphite monochromated Mo $K\alpha$ radiation (λ = 0.71073 Å) on an Oxford Diffraction Xcalibur Gemini single crystal X-ray diffractometer. The CrysAlisPro software [63] was used for data collection, reduction and absorption correction. The structures of all three complexes were solved by direct method and refined on F^2 by full-matrix least-squares procedures. All non-hydrogen atoms were refined anisotropically. The hydrogen atom of the N–H group of $(HL^2)^-$ in **2**·Me_2NCHO was located in a difference map and refined isotropically with restrained thermal parameter. The remaining hydrogen atoms in **2**·Me_2NCHO and all the hydrogen atoms in **3** and **4** were included at ideal positions for structure factor calculation by using a riding model. The SHELX-97 programs [64] available in the WinGX package [65] were used for structure solution and refinement. The Platon [66] and Mercury [67] packages were used for molecular graphics. Selected crystallographic data are summarized in Table 1.

3. Results and discussion

3.1. Synthesis and characterization

The Schiff bases (H_2L^n) were synthesized in 80–90% yields by condensation of the corresponding 4-*R*-1-naphthaldehyde and benzoylhydrazine in 1:1 mole ratio in presence of a few drops of acetic acid in ethanol. The elemental analysis, LCMS and ^{1}H NMR spectra of H_2L^1 and H_2L^2 are consistent with their structures. Treatment of one mole equivalent each of H_2L^n and $NaOAc\cdot 3H_2O$ with Li_2PdCl_4 (generated in situ from $PdCl_2$ and LiCl in 1:2 mole ratio) in methanol afforded the complexes of formula $[Pd(HL^n)Cl]$ in very good yields (80%). Reaction of $[Pd(HL^n)Cl]$ (**1** and **2**) with PPh_3 in 1:2 mole ratio in acetone produced $[Pd(L^n)(PPh_3)]$ (**3** and **4**) in ~70% yields (Scheme 1). The elemental analysis data of each of **1**–**4** support the corresponding molecular formula. All the complexes are yellowish-green and diamagnetic. Both **1** and **2** are sparingly soluble in halogenated solvents like dichloromethane and chloroform, moderately soluble in acetonitrile and acetone and highly soluble in dimethylsulfoxide and dimethylformamide. Solubility behaviour of **3** and **4** is very similar to that of **1** and **2** except for their high solubility in dichloromethane and chloroform also. In solution, all the complexes behave as non-electrolyte.

3.2. Spectroscopic characteristics

Infrared spectra of the Schiff bases (H_2L^1 and H_2L^2) and the corresponding complexes (**1**–**4**) have been collected using KBr pellets. The Schiff bases display two medium intensity bands at ~3223 and ~3062 cm^{-1} due to the amide N–H and the aromatic C–H stretches, respectively. The amide C=O stretch appears as a strong band at 1645 and 1651 cm^{-1} for H_2L^1 and H_2L^2, respectively. The strong band observed at 1576 and 1580 cm^{-1} for H_2L^1 and H_2L^2, respectively is attributed to the C=N stretch [36–41]. As observed for H_2L^1 and H_2L^2, both **1** and **2** also display two bands at ~3180 and ~3040 cm^{-1} due to the amide N–H and the aromatic C–H stretches, respectively. The O-coordinated amide C=O and N-coordinated C=N stretches of the tridentate ligand $(HL^n)^-$ in **1** and **2** appear at ~1600 and ~1560 cm^{-1}, respectively. Both **3** and **4** do not display any band assignable to the N–H or C=O indicating the deprotonation of the amide functionality. The band observed at ~3050 cm^{-1} for **3** and **4** is because of the aromatic C–H moieties of the ligands. Both complexes display a strong band at ~1550 cm^{-1} due to the conjugated C=N–N=C fragment of the tridentate $(L^n)^{2-}$ [36–41].

Electronic spectra of the Schiff bases (H_2L^1 and H_2L^2) and the complexes (**1**–**4**) were recorded using their dimethylformamide solutions. Representative spectra are illustrated in Fig. 1. The spectra of H_2L^1 and H_2L^2 are very similar and exhibit an intense absorption at 336 and 350 nm, respectively. This absorption is flanked by two shoulders at 355 and 320 nm and 370 and 335 nm for H_2L^1 and H_2L^2, respectively. Thus there is a red-shift of the band positions from the unsubstituted H_2L^1 to the substituted H_2L^2. The spectral profiles of **1**–**4** are also very similar. All of them display closely spaced three sharp absorptions followed by two shoulders in the wavelength range 438–345 nm (Fig. 1). In addition to this group of five absorptions, each complex shows two more absorption at ~318 and ~271 nm. It may be noted that the spectrum reported for naphthalene in cyclohexane shows a similar group of absorptions centred at ~275 nm and a high energy shoulder at ~225 nm [68]. Thus the absorption bands of **1**–**4** are primarily due to ligand centred transitions only. As observed for the Schiff bases, here also the absorption features of **2** and **4** are red-shifted compared to those of **1** and **3**. The spectral profiles and the red-shift of band positions observed for H_2L^1, H_2L^2 and the complexes **1**–**4** strongly resemble the spectral characteristics of the

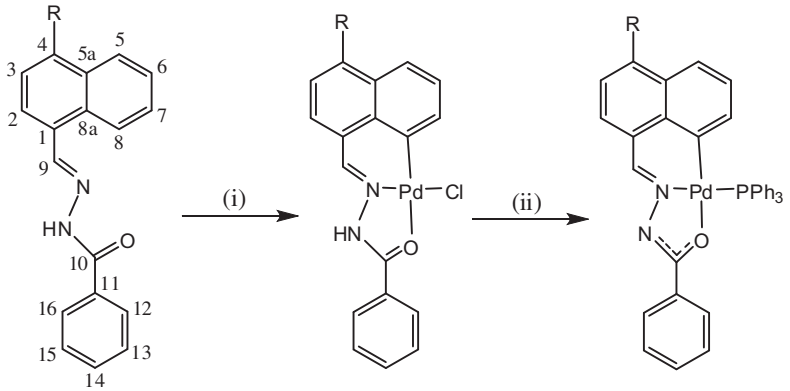

H_2L^n
R = H (n = 1) and OMe (n = 2)

1 (R = H)
2 (R = OMe)

3 (R = H)
4 (R = OMe)

Scheme 1. (i) Li_2PdCl_4 and $NaOAc\cdot 3H_2O$ (equimolar amounts of each in methanol), (ii) PPh_3 (2 mole equivalents in acetone).

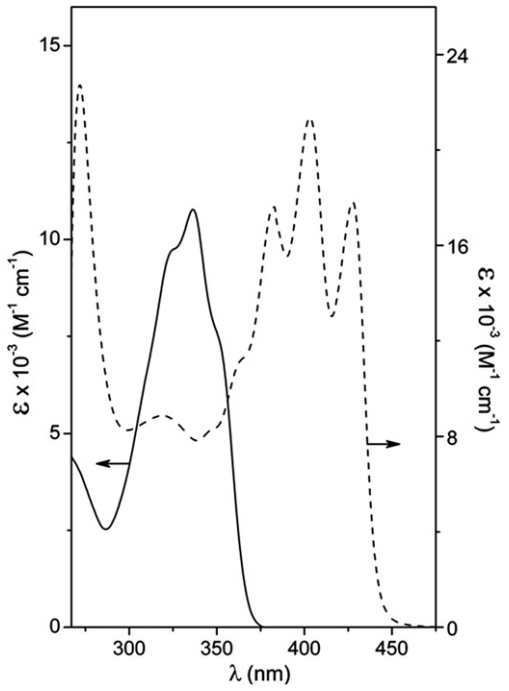

Fig. 1. Electronic spectra of H_2L^1 (—) and $[Pd(L^1)(PPh_3)]$ (**3**) (– –) in dimethylformamide.

corresponding 9-anthracenyl analogues [41]. Alteration of the π–π* energy gaps and hence red-shift of arene absorption bands due to introduction of substituent and also metal coordination is reported in literature [41,69–71].

Table 2
Selected bond lengths (Å) and angles (°) for **2**·Me_2NCHO, **3** and **4**.

Complex **2**			
Pd(1)–C(1)	1.975(5)	Pd(1)–N(1)	1.963(4)
Pd(1)–O(1)	2.132(3)	Pd(1)–Cl(1)	2.3090(15)
C(1)–Pd(1)–N(1)	93.12(19)	C(1)–Pd(1)–O(1)	171.09(17)
C(1)–Pd(1)–Cl(1)	98.06(15)	N(1)–Pd(1)–O(1)	78.58(15)
N(1)–Pd(1)–Cl(1)	168.59(13)	O(1)–Pd(1)–Cl(1)	90.38(10)
Complex **3**			
Molecule 1			
Pd(1)–C(1)	2.020(4)	Pd(1)–N(1)	2.008(3)
Pd(1)–O(1)	2.082(3)	Pd(1)–P(1)	2.2997(10)
C(1)–Pd(1)–N(1)	92.59(14)	C(1)–Pd(1)–O(1)	169.15(12)
C(1)–Pd(1)–P(1)	98.14(11)	N(1)–Pd(1)–O(1)	78.33(11)
N(1)–Pd(1)–P(1)	168.43(9)	O(1)–Pd(1)–P(1)	91.41(7)
Molecule 2			
Pd(2)–C(37)	2.021(4)	Pd(2)–N(3)	2.006(3)
Pd(2)–O(2)	2.078(2)	Pd(2)–P(2)	2.2952(10)
C(37)–Pd(2)–N(3)	92.78(13)	C(37)–Pd(2)–O(2)	169.78(12)
C(37)–Pd(2)–P(2)	97.75(10)	N(3)–Pd(2)–O(2)	78.00(11)
N(3)–Pd(2)–P(2)	168.96(9)	O(2)–Pd(2)–P(2)	91.74(7)
Complex **4**			
Molecule 1			
Pd(1)–C(1)	2.004(3)	Pd(1)–N(1)	1.998(2)
Pd(1)–O(1)	2.077(2)	Pd(1)–P(1)	2.2923(8)
C(1)–Pd(1)–N(1)	93.00(11)	C(1)–Pd(1)–O(1)	168.48(10)
C(1)–Pd(1)–P(1)	99.02(9)	N(1)–Pd(1)–O(1)	78.18(9)
N(1)–Pd(1)–P(1)	166.16(8)	O(1)–Pd(1)–P(1)	90.69(6)
Molecule 2			
Pd(2)–C(38)	2.010(3)	Pd(2)–N(3)	1.997(2)
Pd(2)–O(3)	2.087(2)	Pd(2)–P(2)	2.2905(8)
C(38)–Pd(2)–N(3)	93.05(12)	C(38)–Pd(2)–O(3)	169.68(10)
C(38)–Pd(2)–P(2)	97.52(9)	N(3)–Pd(2)–O(3)	77.82(10)
N(3)–Pd(2)–P(2)	166.97(8)	O(3)–Pd(2)–P(2)	92.19(6)

Dimethylsulphoxide-d_6 solutions of H_2L^1, H_2L^2 and the complexes **1**–**4** were used to record the proton NMR spectra. The spectra of **1** and **2** display all the protons of $(HL^n)^-$, while in the spectra of **3** and **4** some of the aromatic protons of $(L^n)^{2-}$ could not be assigned due to the overlapping signals of the PPh_3 phenyl ring protons. The H^8 proton of H_2L^1 and H_2L^2 resonates as a doublet at δ 7.97 and δ 7.87, respectively. The absence of any such signal in the spectra of **1**–**4** indicates metallation at C8. The signal corresponding to the N–H proton of H_2L^1 and H_2L^2 is observed at δ 11.99 and δ 11.83, respectively. A broad weak signal exhibited by **1** and **2** at δ 14.05 and δ 14.17, respectively is assigned to the N–H proton of $(HL^n)^-$. No such signal in the spectra of **3** and **4** indicates the deprotonation of the amide functionality and the dianionic form ($(L^n)^{2-}$) of the ligand. A singlet observed in the range δ 4.05–4.11 for H_2L^2, **2** and **4** is attributed to the methyl protons of the –OMe substituent. The singlet corresponding to the azomethine proton (H^9) resonates at δ 9.16 and δ 9.00 for H_2L^1 and H_2L^2, respectively, and within δ 8.88–9.07 for **1**–**4**. There is an upfield shift of H^2, H^6 and H^9 protons of the complexes when compared with the corresponding protons of the free Schiff bases. On the other hand, H^3 and H^7 protons of the complexes are shifted downfield and H^5 does not show any significant change. In the benzoyl fragment of **1**–**4**, *ortho* protons (H^{12} and H^{16}) are slightly downfield shifted, while no shift is observed in case of *meta* and *para* protons (H^{13}, H^{14} and H^{15}). ^{31}P NMR spectra of **3** and **4** display a singlet at δ ~25.5 indicating PPh_3 coordination to the metal centre.

3.3. X-ray structures

The molecular structures of **2**, **3** and **4** are confirmed by single crystal X-ray crystallography. Despite our best attempts X-ray quality crystals of **1** could not be grown. The asymmetric unit of **2** contains one complex molecule and one dimethylformamide

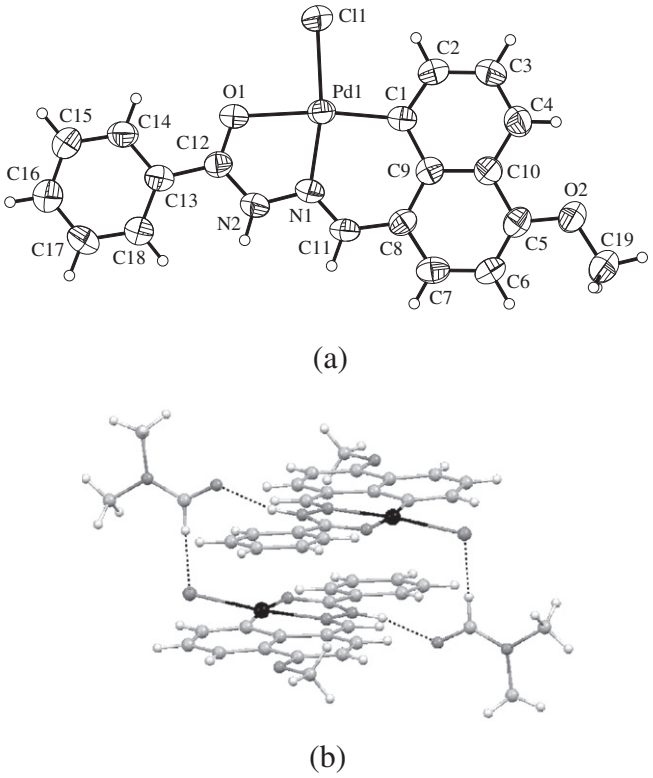

Fig. 2. (a) Molecular structure of **2** with the atom labelling scheme. All non-hydrogen atoms are represented by their 50% probability thermal ellipsoids. (b) Ball and stick diagram of the hydrogen bonded dimer of **2**·Me_2NCHO.

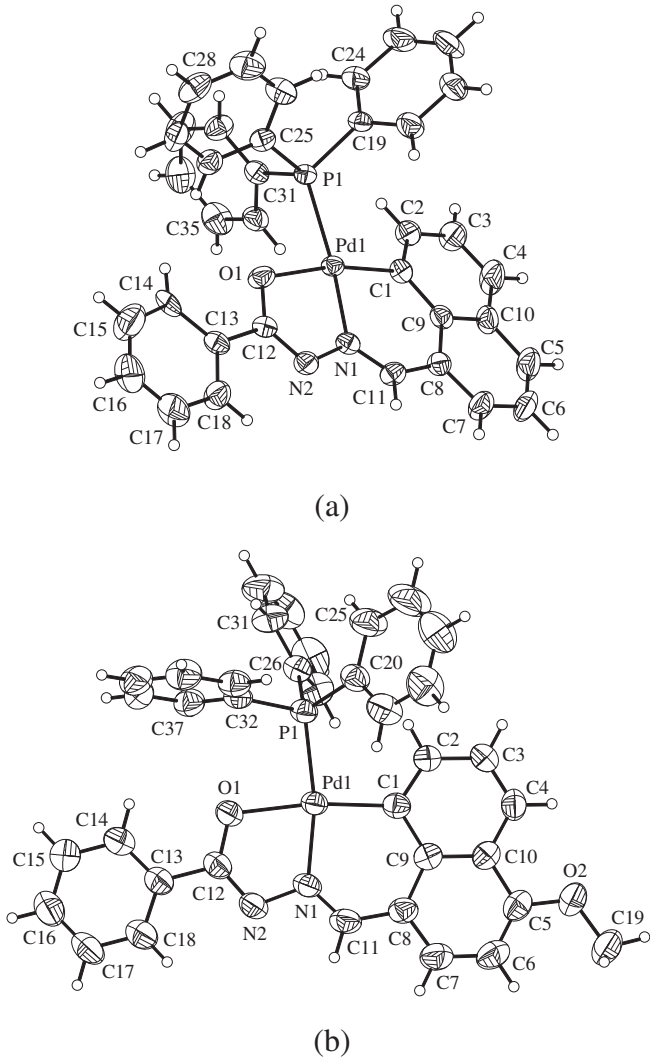

Fig. 3. Molecular structures of (a) **3** and (b) **4** with the atom labelling schemes. For clarity selected C-atoms of the PPh_3 in each structure are labelled. All non-hydrogen atoms are represented by their 50% probability thermal ellipsoids.

molecule, while that of each of **3** and **4** contains two complex molecules. The bond parameters involving the metal centre for all three structures are listed in Table 2. There is no significant variation in the bond parameters of the two molecules present in the asymmetric unit of each of **3** and **4**. The solvated **2**·Me_2NCHO unit dimerizes due to two types of hydrogen bonding. These hydrogen bonds are between the tridentate ligand N–H and the solvent amide-O and between the solvent C–H and the coordinated Cl. In these N–H···O and C–H···Cl interactions, N···O and C···Cl distances are 2.709(6) and 3.620(8) Å, respectively and N–H···O and C–H···Cl angles are 163(5) and 146°, respectively. The structure of **2** and the dimer of the solvate **2**·Me_2NCHO are illustrated in Fig. 2. For each of **3** and **4**, the structure of only one of the two molecules present in the corresponding asymmetric unit is shown in Fig. 3. The $(HL^2)^-$ binds the metal atom through the 1-naphthalenyl *peri*-C, the azomethine-N and the amide-O atoms in **2**, while the metal atom is coordinated to the 1-naphthalenyl *peri*-C, the azomethine-N and the amidate-O atoms of $(L^n)^{2-}$ in each of **3** and **4**. The fourth coordination site in **2** is occupied by a Cl-atom, whereas that in each of **3** and **4** is occupied by the P-atom of a PPh_3 molecule. In each of the three complexes, the four coordinating atoms form a satisfactory square-plane (mean deviation 0.05–0.13 Å) around the metal centre and there is essentially no deviation (0.01–0.04 Å) of the metal centre from this square-plane. The tridentate ligand forms 6,5-fused chelate rings in each of **2**, **3** and **4**. The two chelate rings are slightly folded along the metal and azomethine–N bond (Figs. 2 and 3). The fold angles are within 3.1(2)–6.5(1)°. The C–O and C–N bond lengths of the amide fragment of the tridentate ligand in **2** are 1.241(6) and 1.341(6) Å, respectively, while in **3** and **4** they are within 1.293(4)–1.298(4) and 1.298(4)–1.311(4) Å, respectively. Thus the amide functionality in **2** is protonated and that in **3** and **4** is deprotonated and the negative charge is delocalized over OCN fragment [36–41]. This is also reflected in the significantly longer Pd–O bond length in **2** than that in both **3** and **4** (Table 2). The Pd–N bond length in **4** is longer compared to that in **2** due to the better *trans* directing ability of PPh_3 than chloride. The Pd–C bond lengths (2.004(3)–2.021(4) Å) in **3** and **4** are also longer than that (1.975(5) Å) in **2**. It is very likely that this difference in Pd–C bond lengths is the result of larger *trans* effect of amidate-O in **3** and **4** than the *trans* effect of amide-O in **2** [41]. The Pd–Cl (in **2**) and the Pd–P (in **3** and **4**) bond lengths are unexceptional. In general, all the bond lengths associated with the metal atom in each of **2**, **3** and **4** are within the ranges observed for Pd(II) complexes having similar coordinating atoms [36,37,40–42,48,51–53,55].

4. Conclusions

Cyclometallated complexes [Pd(HL^n)Cl] (**1** and **2**) and [Pd(L^n)(PPh_3)] (**3** and **4**) with the C,N,O-donor Schiff bases 4-*R*-1-naphthaldehyde benzoylhydrazones (H_2L^n, R = H (n = 1) and OMe (n = 2)) have been synthesized and characterized. In each species, *peri* position in preference to the *ortho* position of 1-naphthalenyl fragment of the tridentate ligand is metallated. This regioselective metallation in **1**–**4** has been authenticated by proton NMR and single crystal X-ray crystallography. Currently we are working on synthesis and characterization of other platinum group metal complexes with the present Schiff base system and analogous species containing various polycyclic aromatic moieties to explore and understand the regioselective cyclometallation process.

Acknowledgements

Financial assistance for this work has been received from the Department of Science and Technology (DST) (IYC Grant No. IR/S1/CF-01E/2011). A. R. B. Rao thanks the Council of Scientific and Industrial Research (CSIR) for a research fellowship. We thank the DST and the University Grants Commission (UGC) for the facilities provided under the FIST and the CAS programs, respectively.

Appendix A. Supplementary material

CCDC 916284–916286 contain the supplementary crystallographic data for **2**·Me_2NCHO, **3** and **4**, respectively. These data can be obtained free of charge from The Cambridge Crystallographic Data Centre via www.ccdc.cam.ac.uk/data_request/cif.

References

[1] M.P. Munoz, B. Martin-Matute, C. Fernandez-Rivas, D.J. Cardenas, A.M. Echavarren, Adv. Synth. Catal. 343 (2001) 338–342.
[2] A. Schnyder, A.F. Indolese, M. Studer, H.-U. Blaser, Angew. Chem. Int. Ed. 41 (2002) 3668–3671.
[3] J. Bravo, C. Cativiela, R. Navarro, E.P. Urriolabeitia, J. Organomet. Chem. 650 (2002) 157–172.
[4] C.S. Consorti, M.L. Zanini, S. Leal, G. Ebeling, J. Duport, Org. Lett. 5 (2003) 983–986.
[5] J. Dupont, C.S. Consorti, J. Spencer, Chem. Rev. 105 (2005) 2527–2572.
[6] J. Spencer, D.P. Sharratt, J. Duport, A.L. Monteiro, V.I. Reis, M.P. Stracke, F. Rominger, I.M. McDonald, Organometallics 24 (2005) 5665–5672.

[7] A.D. Raybov, Synthesis (1985) 233–252.
[8] D.C.R. Hockless, R.C. Mayadunne, B. Wild, Tetrahedron: Asymmetry 6 (1995) 3031–3037.
[9] L.E. Overman, T.P. Remarchuk, J. Am. Chem. Soc. 124 (2002) 12–13.
[10] B.J. Burke, L.E. Overman, J. Am. Chem. Soc. 126 (2004) 16820–16833.
[11] I. Aiello, D. Dattilo, M. Ghedini, A. Bruno, R. Termine, A. Golemme, Adv. Mater. 14 (2002) 1233–1236.
[12] B.W. D'Andrade, J. Books, V. Adamovich, M.E. Thompson, S.R. Forrest, Adv. Mater. 14 (2002) 1032–1036.
[13] R.C. Evans, P. Douglas, C.J. Winscom, Coord. Chem. Rev. 250 (2006) 2093–2126.
[14] J. Kalinowski, V. Fattori, M. Cocchi, J.A.G. Williams, Coord. Chem. Rev. 255 (2011) 2401–2425.
[15] I. Omae, Chem. Rev. 79 (1979) 287–321.
[16] A.D. Ryabov, Chem. Rev. 90 (1990) 403–424.
[17] I. Omae, Coord. Chem. Rev. 248 (2004) 995–1023.
[18] M. Ghedini, I. Aiello, A. Crispini, A. Golemme, M.L. Deda, D. Pucci, Coord. Chem. Rev. 250 (2006) 1373–1390.
[19] J. Dupont, M. Pfeffer (Eds.), Palladacycles: Synthesis, Characterization and Applications, Wiley-VCH, Weinheim, 2008.
[20] C.H. Jun, J.B. Hong, Y.H. Kim, K.Y. Chung, Angew. Chem. Int. Ed. 39 (2000) 3440–3442.
[21] Y.G. Lim, J.S. Han, B.T. Koo, J.B. Kang, J. Mol. Catal. A: Chem. 209 (2004) 41–49.
[22] E.J. Yoo, M. Wasa, J.Q. Yu, J. Am. Chem. Soc. 132 (2010) 17378–17380.
[23] C. Zhu, W. Xie, J.R. Falck, Chem. Eur. J. 17 (2011) 12591–12595.
[24] M. Albrecht, G. van Koten, Angew. Chem. Int. Ed. 40 (2001) 3750–3781.
[25] D. Morales-Morales, C.M. Jensen, The Chemistry of Pincer Compounds, Elsevier, Amsterdam, 2007.
[26] W. Leis, H.A. Mayer, W.C. Kaska, Coord. Chem. Rev. 252 (2008) 1787–1797.
[27] N. Selander, K.J. Szabó, Chem. Rev. 111 (2011) 2048–2076.
[28] J.-L. Niu, X.-Q. Hao, J.-F. Gong, M.-P. Song, Dalton Trans. 40 (2011) 5135–5150.
[29] G. van Koten (Ed.), Organometallic Pincer Chemistry, in: D. Milstein (Ed.), Topics in Organometallic Chemistry, vol. 40, Springer, Heidelberg, 2013.
[30] C.S. Consorti, G. Ebeling, F. Rodembusch, V. Stefani, P.R. Livotto, F. Rominger, F.H. Quina, C. Yihwa, J. Dupont, Inorg. Chem. 43 (2004) 530–536.
[31] C.S. Consorti, G. Ebeling, F.R. Flores, F. Rominger, J. Dupont, Adv. Synth. Catal. 346 (2004) 617–624.
[32] J. Vicente, J.-A. Abad, J. López-Serrano, P.G. Jones, C. Nájera, L. Botella-Sergura, Organometallics 24 (2005) 5044–5057.
[33] J. Storch, J. Čermák, M. Pošta, J. Sýkora, I. Císařová, J. Organomet. Chem. 693 (2008) 3029–3034.
[34] B. Vabre, Y. Canac, C. Duhayon, R. Chauvin, D. Zargarian, Chem. Commun. 48 (2012) 10446–10448.
[35] G.R. Rosa, D.S. Rosa, RSC Adv. 2 (2012) 5080–5083.
[36] S. Das, S. Pal, J. Organomet. Chem. 689 (2004) 352–360.
[37] S. Das, S. Pal, J. Organomet. Chem. 691 (2006) 2575–2583.
[38] R. Raveendran, S. Pal, J. Organomet. Chem. 692 (2007) 824–830.
[39] R. Raveendran, S. Pal, J. Organomet. Chem. 694 (2009) 1482–1486.
[40] A.R.B. Rao, S. Pal, J. Organomet. Chem. 696 (2011) 2660–2664.
[41] A.R.B. Rao, S. Pal, J. Organomet. Chem. 701 (2012) 62–67.
[42] J. Granell, R. Moragas, J. Sales, M. Font-Bardía, X. Solans, J. Chem. Soc., Dalton Trans. (1993) 1237–1244.
[43] Y.-F. Han, H. Li, P. Hu, G.-X. Jin, Organometallics 30 (2011) 905–911.
[44] A.J. Klaus, P. Rys, Helv. Chim. Acta 64 (1981) 1452–1466.
[45] M. Hugentobler, A.J. Klaus, H. Mettler, P. Rys, G. Wehrle, Helv. Chim. Acta 65 (1982) 1202–1211.
[46] R. Annunziata, S. Cenini, F. Demartin, G. Palmisano, S. Tollari, J. Organomet. Chem. 496 (1995) C1–C3.
[47] M. Crespo, M. Font-Bardía, S. Pérez, X. Solans, J. Organomet. Chem. 642 (2002) 171–178.
[48] Y. Li, K.-H. Ng, S. Selvaratnam, G.-K. Tan, J.J. Vittal, P.-H. Leung, Organometallics 22 (2003) 834–842.
[49] R. Bhawmick, P. Das, D.N. Neogi, P. Bandyopadyay, Polyhedron 25 (2006) 1177–1181.
[50] L. Kind, A.J. Klaus, P. Rys, V. Gramlich, Helv. Chim. Acta 81 (1998) 307–316.
[51] S. Lentijo, J.A. Miguel, P. Espinet, Organometallics 30 (2011) 1059–1066.
[52] S. Lentijo, J.A. Miguel, P. Espinet, Dalton Trans. 40 (2011) 7602–7609.
[53] S. Tollari, G. Palmisano, F. Dematrin, M. Grassi, S. Magnaghi, S. Cenini, J. Organomet. Chem. 488 (1995) 79–83.
[54] M. Crespo, E. Evangelio, J. Organomet. Chem. 689 (2004) 1956–1964.
[55] D.N. Neogi, P. Das, A.N. Biswas, P. Bandyopadhyay, Polyhedron 25 (2006) 2149–2152.
[56] D.N. Neogi, A.N. Biswas, P. Das, R. Bhawmick, P. Bandyopadhyay, Inorg. Chim. Acta 360 (2007) 2181–2186.
[57] A.N. Biswas, P. Das, V. Bagchi, A. Choudhury, P. Bandyopadhyay, Eur. J. Inorg. Chem. (2011) 3739–3748.
[58] A.N. Biswas, P. Das, S. Sengupta, A. Choudhury, P. Bandyopadhyay, RSC Adv. 1 (2011) 1279–1286.
[59] D.N. Neogi, A.N. Biswas, P. Das, R. Bhawmick, P. Bandyopadhyay, J. Organomet. Chem. 724 (2013) 147–154.
[60] D.D. Perrin, W.L.F. Armarego, D.P. Perrin, Purification of Laboratory Chemicals, second ed., Pergamon, Oxford, 1983.
[61] SMART Version 5.630 and SAINT-plus Version 6.45, Bruker-Nonius Analytical X-ray Systems Inc., Madison, WI, USA, 2003.
[62] G.M. Sheldrick, SADABS, Program for Area Detector Absorption Correction, University of Göttingen, Göttingen, Germany, 1997.
[63] CrysAlisPro Version 1.171.33.55, Oxford Diffraction Ltd., Abingdon, Oxfordshire, UK, 2007.
[64] G.M. Sheldrick, XHELX-97, Structure Determination Software, University of Göttingen, Göttingen, Germany, 1997.
[65] L.J. Farrugia, J. Appl. Crystallogr. 32 (1999) 837–838.
[66] A.L. Spek, Platon, A Multipurpose Crystallographic Tool, Utrecht University, Utrecht, The Netherlands, 2002.
[67] C.F. Macrae, I.J. Bruno, J.A. Chisholm, P.R. Edgington, P. McCabe, E. Pidcock, L. Rodriguez-Monge, R. Taylor, J. van de Streek, P.A. Wood, J. Appl. Crystallogr. 41 (2008) 466–470.
[68] J.M. Dixon, M. Taniguchi, J.S. Lindsey, Photochem. Photobiol. 81 (2005) 212–213.
[69] S. Suzuki, T. Fuji, T. Ishikawa, J. Mol. Spectrosc. 57 (1975) 490–499.
[70] L. Cuffe, R.D.A. Hudson, J.F. Gallagher, S. Jennings, C.J. McAdam, R.B.T. Connelly, A.R. Manning, B.H. Robinson, J. Simpson, Organometallics 24 (2005) 2051–2060.
[71] Y.-Y. Liu, M. Grzywa, M. Tonigold, G. Sastre, T. Schüttrigkeit, N.S. Leeson, D. Volkmer, Dalton Trans. 40 (2011) 5926–5938.